A Cold Heat Transfer Tunnel Employing Liquid Crystals for Measuring Full Surface Heat Transfer Coefficients over Turbine Blade Passages.

P. T. Ireland Z. Wang T. V. Jones
A. R. Byerley
Department of Engineering Science
University of Oxford
Parks Road
Oxford
OX1 3JP

March, 1988

Abstract

The cold heat transfer cascade tunnel and the use of liquid crystals in the measurement are described. The technique is based on previous work by the authors and this is reviewed. Results from a cascade tunnel are presented. These demonstrate the powerful nature of this research tool in its ability to examine the detailed heat transfer distributions associated with passage secondary flow and other turbine phenomena.

1 Introduction

Although much progress has been made in the analysis of heat transfer levels over turbine blading in regions where the flow field is predominantly two dimensional, the calculation of heat loads at the roots and tips of the aerofoils and over the passage endwalls remains one of the most severe tests of predictive methods. In these regions, heat transfer is dominated by a complex system of secondary flows which result in heat transfer coefficient distributions with high spatial gradients. The advantages of a method which yields detailed measurements over the full surface of the cascade are then apparent. The work reported here is the first application of a particular technique which was developed for the measurement of blade internal cooling passage heat transfer coefficients. The results reveal details of the heat transfer coefficient distribution which would not be resolved using discrete gauge measurements. In particular, the 'dual nature' of the horseshoe vortex which forms ahead of the blade leading edge is apparent.

Historically, the technique was first applied to internal flows by Jones et al. [4,6] and has subsequently been used with success by Metzger and Larson [19], and Saabas et al. [21] . Detailed accounts of the application of the transient method to cooling ducts are given in [2,3,9,10,12] and comparisons to steady state heated foil methods have been made by Jones and Hippensteele [15] and more recently by Baughn et al. [1].

c	specific heat capacity of model material
h	heat transfer coefficient
k	thermal conductivity of model material
n	distance into the model material measured normal to the surface
p	pressure surface length
Re_{inlet}	inlet Reynolds number based on true chord
s	suction surface length
t	time
t_1	time for first calibrated colour display
t_2	time for second calibrated colour display
x	distance measured from geometric stagnation line along blade surface
$T(n,t)$	temperature
$T_{crystal}$	calibrated liquid crystal colour display temperature
T_{gas}	gas temperature
$T_{initial}$	temperature before flow initiation
α	thermal diffusivity of model material
ρ	density of model material

Table 1: Nomenclature

2 Experimental Technique

The method measures the surface temperature rise of a model made from a good thermal insulator when subjected to a step in convective heating The test section is initially at a uniform temperature and the surface temperature response is monitored using thermochromic liquid crystals. It can be shown [6,9,12] that under the test conditions, the conduction of heat in a direction parallel to the surface has a negligible effect on the surface temperature rise. The surface temperature history is then governed by the one dimensional transient conduction equation.

$$\frac{\partial^2 T}{\partial n^2} = \frac{1}{\alpha}\frac{\partial T}{\partial t} \tag{1}$$

with the following boundary and initial conditions

$$-k\frac{\partial T}{\partial n}_{n=0} = h(T_{gas} - T_{n=0}) \tag{2}$$

$$-k\frac{\partial T}{\partial n}_{n=\infty} = 0 \tag{3}$$

$$T(n,0) = T_{initial} \tag{4}$$

The solution to these equations for a constant heat transfer coefficient and gas temperature can be written

$$\frac{T_{crystal} - T_{initial}}{T_{gas} - T_{initial}} = 1 - e^{\frac{h^2 t}{\rho c k}} erfc(\frac{h\sqrt{t}}{\sqrt{\rho c k}}) \tag{5}$$

From which it can be seen that, provided T_{gas},$T_{initial}$ and $\sqrt{\rho c k}$ are known, a knowledge of the surface temperature at a particular time after gas flow initiation is sufficient to yield the heat transfer coefficient. Alternatively, the time taken for any point on the surface to

Colour	*Crystal 1*	*Crystal 2*	*Crystal 3*
red	57.1^0C	40.3^0C	30.4^0C
yellow	58.1^0C	40.5^0C	30.7^0C
blue	59.0^0C	40.7^0C	30.9^0C

$T_{initial}$	$57.5°C$
$T^{\bullet}_{gas}$	$17.6°C$
$\sqrt{\rho ck}$	$569.0 W m^{-2} k^{-1} sec^{0.5}$

Table 2: Experimental temperatures and Thermal Product

reach a particular temperature can be used. This latter approach permits a simple sort of surface thermometer to be employed. Originally , [4,6,16,24,17] , researchers applied a coating which melted at an accurately known temperature. The change in the reflectance of light in the visible spectrum at this phase transition was used to depict an isotherm, and by photographing the progress of this line over the model surface, a global map of heat transfer coefficient was obtained.

More recent work has utilised thermochromic liquid crystals to indicate either a series or a single isotherm. These substance selectively scatter light at a preferred wavelength as a function of temperature. As a consequence, they appear to change colour over a certain temperature range. A typical example of a chiral nematic, [18], sort of liquid crystal supplied by BDH[1] appears red at 40.3°C and, as the temperature is increased, passes through the full visible spectrum over a range of 0.5°C (see Table 2).

The accuracy of the measurement is dependent on an adequate liquid crystal frequency response, and earlier tests [11] on the chiral nematic type of liquid crystal employed showed that the time response was of the order of milliseconds. The tests reported here are all long enough for the response of the crystal to be considered instantaneous.

Although it is possible to establish the temperature at any point within the colour display band by monitoring the colour of the coating, [5], it is more accurate in practice, to select a crystal which is optically active over a narrow range of temperature and acquire one reading from a single colour. In situations where more than one temperature is required, combinations of different liquid crystal devices have been employed [3,10,11,12]. This mixing is possible since the crystals are supplied as micro-capsules. The active liquid crystal is in the form of tiny droplets ($10\mu m$ in diameter) encased in a protective shell of gelatin and gum arabic [20]. When applied to the surface, the coating consists of a single layer of capsules containing the required liquid crystal material.

For these tests, a mixture of three different liquid crystals was employed as detailed in Table 2. The higher temperature colour display type with a comparatively wide colour play was used to ensure that the initial surface temperature of the model was uniform. The air flow during the test was drawn from atmosphere ($17.6°C$). Consequently, at any point,two values of the heat transfer coefficient could be calculated from the two times after flow initiation that the surface appeared yellow.

The transient method is equivalent to measuring heat transfer coefficient under isothermal

[1]BDH Ltd,Poole,Dorset BH12 4NN,UK.

Blade dimensions	
Profile scale	1:1
True chord length	69.0 mm
Axial chord length	37.4 mm
Pitch spacing	57.4 mm
Span	50.0 mm
Suction surface length	83.6 mm
Pressure surface length	67.0 mm
Tunnel parameters	
Entry length	270. mm
Inlet velocity	22.5 ms^{-1}
Re_{inlet}	93000
Calculated boundary thickness	8.0mm

Table 3: Cascade Details.

wall conditions. The thermal boundary conditions of the transient technique have been considered in [1,10,12,19]and the data presented over the turbine cascade in the present report was confirmed as being measured for a time invariant heat transfer coefficient. This aspect of the transient method is discussed further in section 4.

3 Experimental Facility and Test Procedure

A schematic diagram of the experimental facility is included as Figure 1. .Initially, the test section was isolated from the vacuum pump by the slide valve. External radiative heaters were positioned around the working section, which is shown in Figure 2., and heated air was ducted through the cascade from an air blower inserted in the tunnel inlet. Details of the blade profile are included in Table 3.

The aerofoil profile has previously been studied by Watt et al. [25] and many of the cascade details in this reference are the same for the current tests. During the warm up phase, the air flow is not recirculated , but leaves the model from a vent which was closed before the main test flow was initiated. Immediately prior to the test, the heaters were removed and the entrance to the tunnel was plugged to allow the perspex temperature to achieve equilibrium. This state was confirmed by monitoring surface temperature thermocouples placed within the working section. The temperature uniformity was ensured by observing the colour display of *Crystal 1.*

Once the surface of the model was at a uniform steady temperature, the plug was rapidly removed and the flow then initiated by the fast acting slide valve. The colour display of the crystal coating was recorded by video cameras during the test. The contours of heat transfer coefficient,Figures 3-5, were obtained by replaying the video recordings and assigning a heat transfer coefficient contour to the position of the yellow display for *Crystal 2* at certain times. Values calculated from *Crystal 3* were also obtained at spot points to check that the assumptions employed in the analysis were vindicated. The values were found to agree within experimental error. For these tests, the greatest experimental uncertainty in the heat transfer data was 6.0%. The analysis used was that given in Appendix 4-B of [12].

Flat plate correlations [22] were used to calculate the turbulent boundary layer thickness (8mm) at a position immediately upstream of the vanes, and to check the heat transfer coefficient at this location. The latter value was found to to be within 10% of the measured heat transfer coefficient.

4 Discussion of Results

The purpose of this work was not to conduct a detailed study of the secondary flows resident in a turbine cascade. Rather, the work aimed to demonstrate that a relatively straightforward experimental method could be used to acquire very detailed full surface heat transfer contours. It is worth emphasising that the technique, as a matter of course, generates complete contours. In other words, the data presented in Figures 3 to 5 have not been numerically smoothed. This ensures that quite subtle features in the lay of the contours are preserved. One such feature, on the endwall near to the blade leading edge, was first observed using the same method under the vortex structure at the front of pedestals used in cooling passages [10,12]. The separation which forms at the junction between the pedestal and the cooling passage wall is strongly related to that ahead of the turbine blade.Both are the result of the incident boundary layer 'rolling up' under the adverse pressure gradient as the flow approaches the obstacle. Under this part of the separation system, heat transfer to the endwall is always found to be highest at the flow attachment point. For a symmetrical body such as a cylinder, this point will be on the line of symmetry, and for the turbine blades will be close to the geometrical stagnation point. Levels of heat transfer coefficient on the endwall then decrease as one moves away from the obstacle (Figure 6). However, at a certain distance from the cylinder, this monotonic decrease is arrested, and a second peak in h is observed [10,12]. Much flow visualisation work for the pedestal established this peak as being at the attachment line of a second vortex ahead of the horseshoe vortex. Flow field studies by other workers [23,14] have also succeeded in classifying the vortex system as being comprised of two main vortices (the 'horseshoe' vortex adjacent to the obstacle, and the 'separation' vortex upstream). In fact a small counter vortex must exist between the two though its influence on heat transfer appears to be insignificant. The first association of the heat transfer distribution to the double main vortex structure is given in [12]. Hippenteele et al. [8] have also observed the same feature around a cascade using a steady state heated coating method [7].

Although flow visualisation would be required for a full discussion of the features observed, it is likely that the pressure side leg of the horseshoe vortex remains close to the blade, and that the attachment line under this vortex is responsible for the bend in the contours adjacent to this surface. Over the pressure surface of the blade, the levels of heat transfer are lower towards the endwall. This tendency of the horseshoe vortex to reduce heat transfer to the obstacle, in this case the blade, near to the junction with the endwall has been observed previously over a pedestal placed in fully developed channel flow [1,10]. It was found that this phenomenon was dependent on the thermal boundary layer in the incident flow. The latter study showed that, when the heat transfer was only to the obstacle itself, the vortex system acted to increase heat transfer in the vicinity of the junction. These thermal boundary conditions were achieved by wrapping an insulated perspex cylinder with an electrical heater but supplying no heat at the windtunnel endwall. Comparison was made to the results of tests using the transient method applied to an identically dimensioned cylinder in the same flow field. In this case, both thermal and hydrodynamic boundary layers were

present in the flow just upstream of the pedestal. Around the front of the pedestal, it was found that the major influence of the vortex system was to reduce heat transfer levels from the mid span values close to the cylinder extremities.

The endwall contours also appear to indicate that the outer separation vortex crosses the passage and comes close to the suction surface of the blade at between 35% and 40% of the suction surface length. Inspection of the suction surface contours ,Figure 5,then reveals evidence of three dimensional effects from about this position. Interestingly, the levels of heat transfer coefficient are ,up until about the 60% line, *increased* from the mid-span values. This is thought to be due to an attachment line between the counter rotating vortices (specifically, the suction surface side leg of the horseshoe vortex, and the pressure side separation vortex which has crossed the passage). As discussed above, if only one vortex is close to the blade, as is the case on the pressure surface , then no such attachment occurs, and heat transfer levels are not necessarily increased - depending on the presence or not of the thermal boundary layer. Beyond 60%, a rise in heat transfer for flow not in the vortex system and away from the endwalls , identified as transition, masks the influence of this line.

Amongst the highest levels of heat transfer to the endwall are those recorded behind the aerofoil in the wake region. It should be stressed that the flow was entirely subsonic and hence this enhancement is *not* associated with any compressible flow phenomena. The results presented are for a single test condition for which both the inlet Reynolds number and Mach number were considerably lower than the design values. Subsequent work, to be reported, has been performed at engine Mach numbers.

The final figure compares values of heat transfer coefficient calculated from the two times t_1 and t_2. It can be seen that the heat transfer coefficient distribution is the same, to within the experimental uncertainty, for both cystals. This would not be the case if the heat transfer coefficient distribution altered with time. The assertion that the change in the upstream wall boundary condition throughout the duration of the transient test, has an insignificant influence on the measured data is thus confirmed. Hence, it is clear that the thermal boundary condition is effectively that of an isothermal wall. In addition, under the test assumptions, it can be shown,[13], that the time ratio $\frac{t_2}{t_1}$ should be the same at all model points. This permits a very easy check of the data to be made at any point on the model surface.

5 Conclusions

The work reported here has demonstrated that a novel method of measuring heat transfer coefficient can be applied successfully to turbine cascades. The advantages of a full surface measurement has been demonstrated by the detail of the contours of heat transfer coefficient presented.

6 Acknowledgements

The authors wish to thank the Royal Aerospace Establishment (Pyestock) for the financial support given to the work reported here. In addition, the technical assistance of Mr. P. J. Timms was much appreciated.

References

[1] Baughn, J W, Ireland, P T, Jones, T V and Sanei, N 1988 A comparison of the transient and heated-coating methods for the measurement of local heat transfer coefficients on a pin fin *ASME paper 88-GT-180*

[2] Byerley, A R B, Ireland, P T and Jones, T V 1988 Detailed heat transfer measurements near and within the entrance of a film cooling hole *ASME paper 88-GT-155*

[3] Byerley, A R B, Ireland, P T and Jones, T V 1988 Detailed heat transfer measurements near the entrance to an inclined film cooling hole inside a gas turbine blade em UK National Heat Transfer Conference, Glasgow, UK, September paper C164/88

[4] Clifford, R J, Jones, T V and Dunne, S T 1983 Techniques for obtaining detailed heat transfer coefficient measurements within gas turbine blade and vane cooling passages *ASME paper 83-GT-58*

[5] Cooper T E, Field, R J and Meyer J F 1975 Liquid crystal thermography and its application to the study of convective heat transfer *ASME Journal of Heat Transfer* vol. 97, pp 442-450

[6] Dunne, S T 1983 A study of flow and heat transfer in gas turbine blade cooling passages *D.Phil. thesis, University of Oxford*

[7] Hippensteele, S A , Russell, L M and Torres F J 1987 Use of a liquid-crystal, heater-element composite for quantitative, high-resolution heat transfer coefficients on a turbine airfoil, including turbulence and surface roughness effects *NASA TM 87355*

[8] Hippensteele, S A , Russell, L M and Torres F J 1987 Evaluation of a method for heat transfer measurements and thermal visualisation using a composite of a heater element and liquid crystals *NASA TM 81639*

[9] Ireland, P T and Jones T V 1985 The measurement of local heat transfer coefficients in blade cooling geometries*AGARD Conf. 390 , Heat Transfer and Cooling in Gas Turbines*

[10] Ireland,P T and Jones T V 1986 Detailed measurements of heat transfer on and around a pedestal in fully developed flow *Proc. 8th Int. Heat Transfer Conf.,San Francisco* (Hemisphere) vol.3 pp 975-80

[11] Ireland,P T and Jones T V 1987 The response time of a surface thermometer employing encapsulated thermochromic liquid crystals *J.Phys. E:Sci.Instrum.* vol.20 pp 1195-1199

[12] Ireland,P T 1987 Internal cooling of turbine blades *D.Phil. thesis, University of Oxford*

[13] Ireland, P T and Jones, T V 1987 Note on the double crystal method of measuring heat transfer coefficient *Oxford University, Department of Engineering Science Report No. 1710/87*

[14] Ishii, J and Honami, S 1985 A three-dimensional turbulent detached flow with a horse-shoe vortex *ASME paper 85-GT-70*

[15] Jones, T V and Hippensteele, S A 1987 High resolution heat-transfer-coefficient maps applicable to compound-curve surfaces using liquid crystals in a transient wind tunnel. *ASME HTD vol. 71 pp 1-9*

[16] Jones, T V and Russell, C M B 1981 Heat transfer coefficients on finned tubes *ASME HTD vol. 21 pp17-25*

[17] Jones, R A and Hunt, J L 1966 Use of fusible temperature indicators for obtaining quantitative aerodynamic heat-transfer data. *NASA TR R-230*

[18] Mc Donnell, D G and Sage, I 1982 New thermochromic liquid crystals *Recent Advances in Medical Thermology, ed. by Ring, E F J and Phillips, B* (New York:Plenum) p. 305

[19] Metzger, D E and Larson, D E 1986 Use of melting point surface coatings for local convection heat transfer measurements in rectangular channel flows with 90-deg turns *ASME Journal of Heat Transfer* vol. 108

[20] Parsley, M 1986 Thermocromic liquid crystals *BDH publication*

[21] Saabas, H J , Arora, S C and Abdel Messeh, W 1987 Application of the transient test technique to measure local heat transfer coefficients associated with augmented airfoil cooling passages*ASME paper 87-GT-212*

[22] Schlichting, H S 1968 Boundary layer theory, Mc Graw-Hill Book Company.

[23] Sieverding, C H 1985, Recent progress in the understanding of basic aspects of secondary flows in turbine passages *Journal of Engineering for Gas Turbines and Power* vol. 107, pp 248-257

[24] Throckmorton, D A and Stone, D R 1974 Model wall and recovery temperature effects on experimental heat-transfer data *AIAA Journal* vol.12, pp 169-170

[25] Watt, R W, Allen, J L, Baines, N C, Simons, J P and George, M 1987 A study of the effects of thermal barrier coating surface roughness on the boundary layer characteristics of gas-turbine aerofoils *ASME paper 87-GT-223*

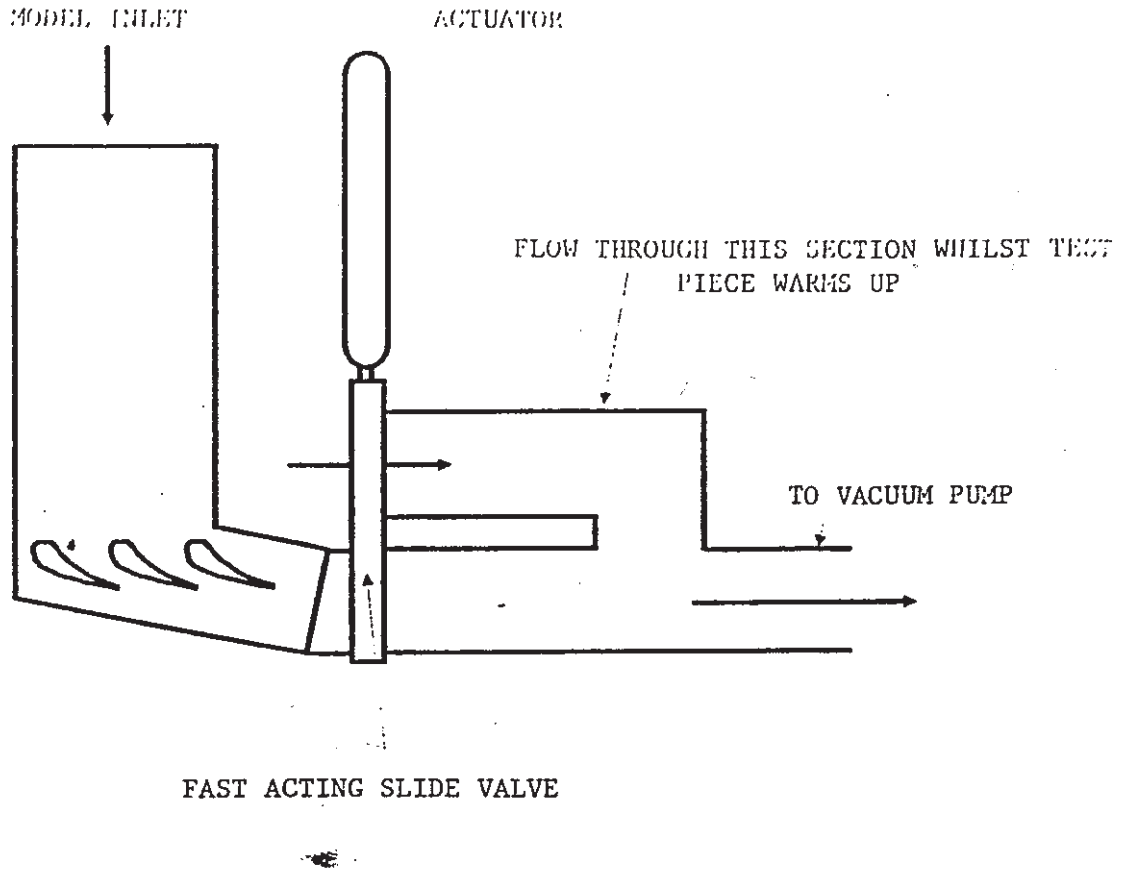

Figure 1: Schematic diagram of the experimental facility.

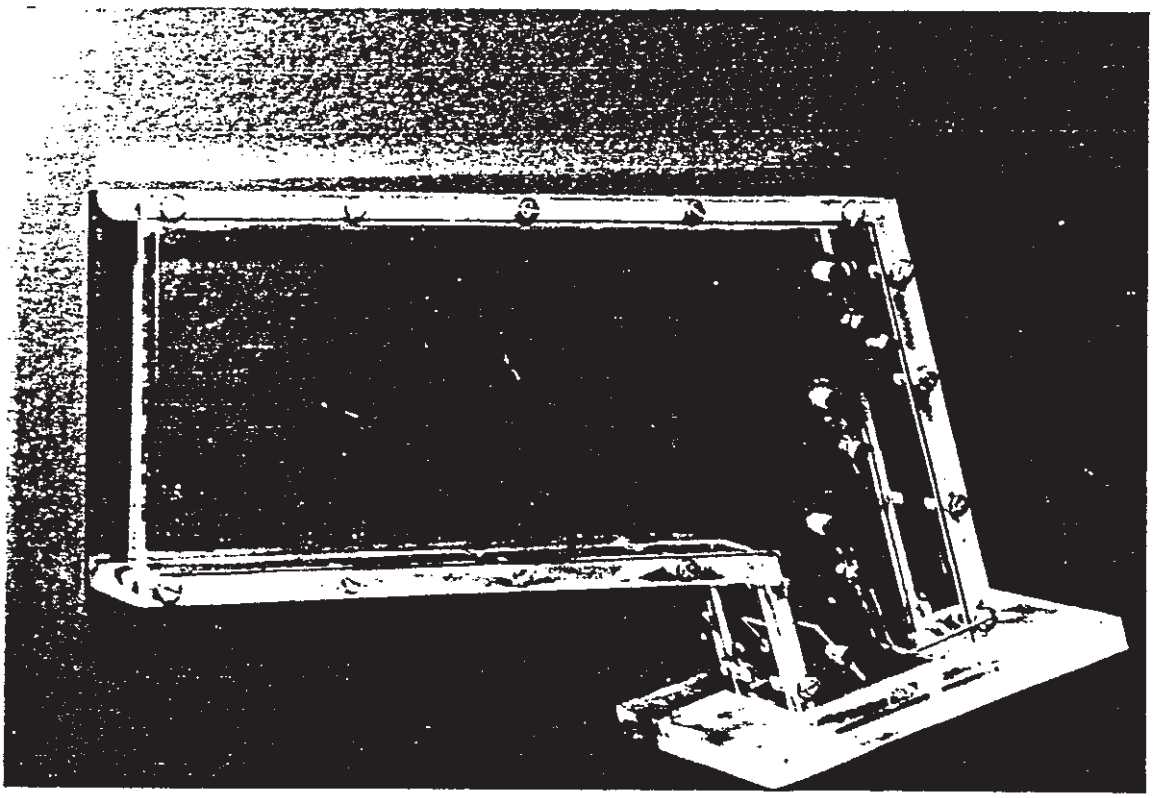

Figure 2: Perspex test section (flow inlet to the left).

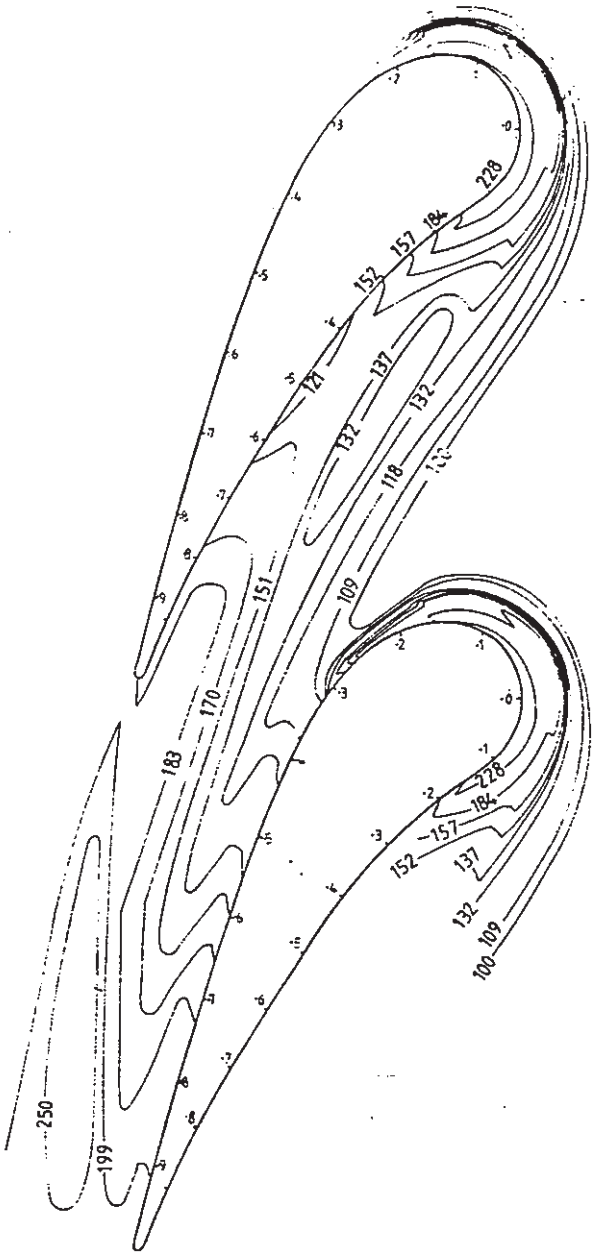

Figure 3: Contours of heat transfer coefficient (W/m/m/k) on the passage endwall. The smaller numbers on the vanes are x/s and x/p on the suction surface and the pressure surface respectively.

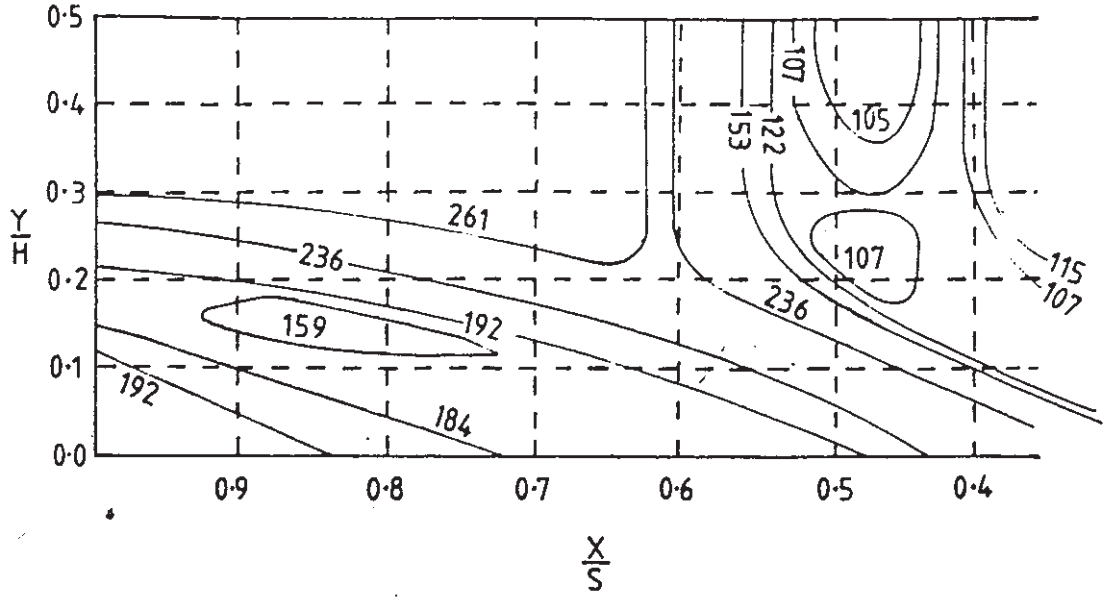

Figure 4: Contours of heat transfer coefficient (W/m/m/k) over the blade suction surface.

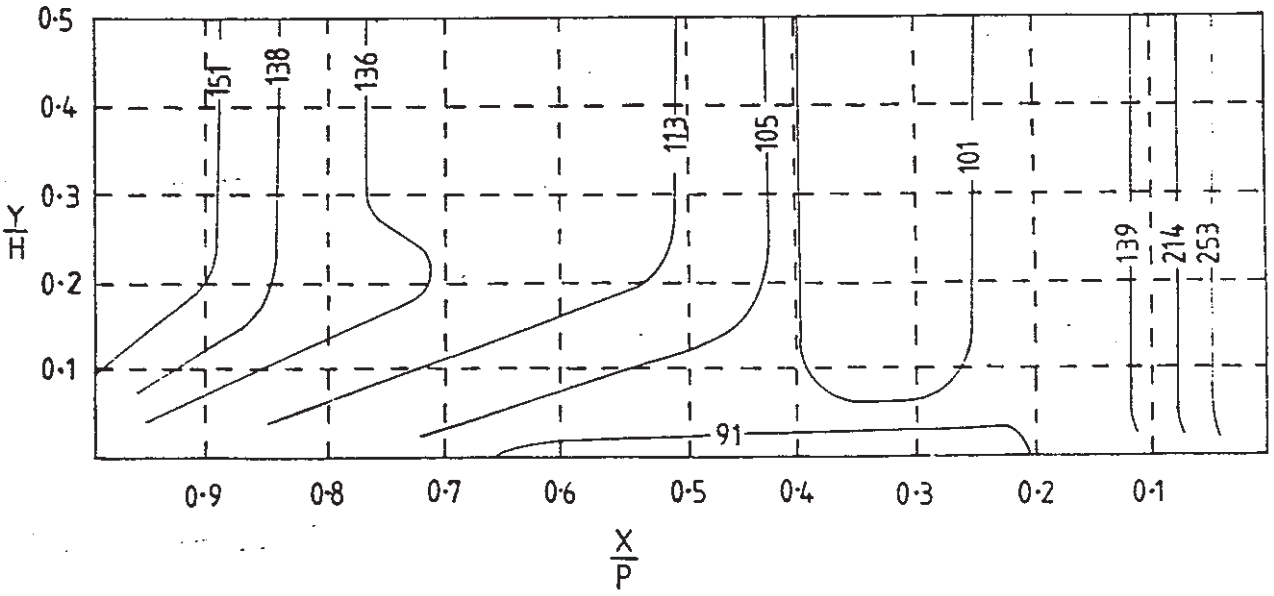

Figure 5: Contours of heat transfer coefficient (W/m/m/k) over the blade pressure surface.

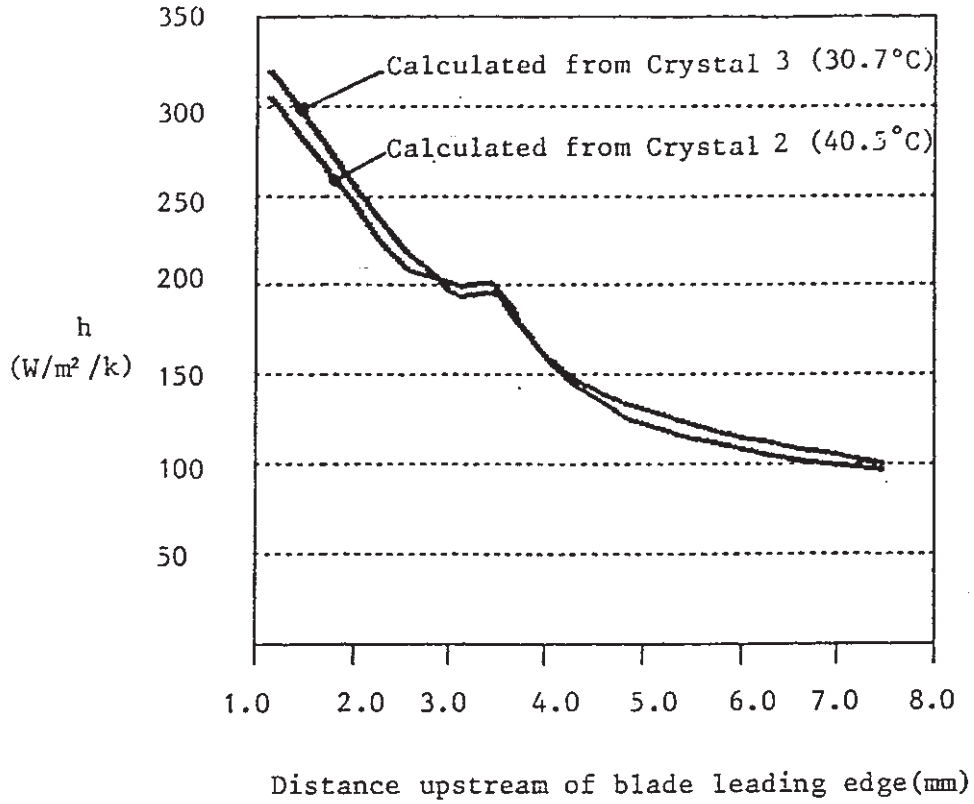

Figure 6: Comparison of heat transfer coefficient calculated on the endwall from the two times that the surface appears yellow. The second peak in h associated with the double vortex structure is apparent at approximately 3.5mm from the blade leading edge.